Hindawi
Advances in Materials Science and Engineering
Volume 2021, Article ID 3024490, 13 pages
https://doi.org/10.1155/2021/3024490

Research Article

Experimental Study on Stiffness Softening of Soil-Rock Mixture Backfill under Metro Train Cyclic Load

Zuliang Zhong,[1,2] **Hong Zou**,[1] **Xiangxiang Hu**,[1] **and Xinrong Liu**[1,2]

[1]*School of Civil Engineering, Chongqing University, Chongqing 400045, China*
[2]*National Joint Engineering Research Center of Geohazard Prevention in Reservoir Area, Chongqing 400045, China*

Correspondence should be addressed to Zuliang Zhong; haiou983@126.com

Received 25 August 2021; Revised 28 September 2021; Accepted 6 October 2021; Published 13 October 2021

Academic Editor: Ivan Giorgio

Due to the thick soil layer, short backfill time, and low degree of consolidation of the soil-rock mixture backfill in Chongqing city, metro train tunnels passing through this type of strata are prone to large settlements during operation, which greatly affects the stability of the tunnel and the safety of metro train operations. In response to this problem, the dynamic triaxial test of the soil-rock mixture backfill under cyclic loading was carried out to study the dynamic characteristics of the soil-rock mixture backfill under cyclic loading. The effect of initial consolidation degree, effective consolidation confining pressure, and rock content on the stiffness softening of soil-rock mixture backfill was analyzed. The results show that the initial consolidation degree, effective consolidation confining pressure, and rock content are all important factors affecting the stiffness of soil-rock mixture backfill under cyclic loading. As the number of cycles increases, the lower the initial consolidation degree and effective consolidation confining pressure, the faster the attenuation of the softening index, and the larger the amplitude. As the rock content increases, the softening index increases and the stiffness of the backfill changes from softening to hardening. Based on the test data, the softening-hardening model of the soil-rock mixture is established, which is in good agreement with the field test results. This study can provide a reference for predicting and controlling the postconstruction settlement of the metro tunnel in the soil-rock mixture backfill.

1. Introduction

Soil-rock mixture backfill is a nonuniform loose soil media system with a certain rock content, which consists of high strength rock, fine soil, and pores with a certain engineering scale. In the early construction of mountainous cities, mountains are excavated and valleys are filled to form a large area of soil-rock mixture backfilling area. With the expansion and acceleration of urbanization, metro trains will inevitably pass through the soil-rock mixture backfill. The soil-rock mixture has the typical characteristics of loose structure, large porosity, weak cementing ability, poor stability, and strong permeability. The construction and operation of metro tunnels will subject to various safety hazards, including large deformation, uneven settlement, collapse, and water seepage in karst caves. According to the principle of effective stress, the excess pore pressure of the soil-rock mixture under the cyclic loading of metro trains will increase and the effective stress will decrease. The reduction in the strength and stability of the soil-rock mixture will cause large deformation of the surrounding rock of the metro tunnel in the backfill area [1–3].

Previous studies mainly focused on the softening characteristics of soil stiffness under cyclic loading. Most of the research objects are sandy soil, silt, and clay [4–8]. However, there are few studies on the stiffness softening characteristics of soil-rock mixtures. The effect of confining pressure, cyclic load amplitude, drainage conditions, saturation, and initial compactness on the cumulative strain, resilience characteristics, and particle breakage of coarse-grained soil was analyzed [9–12]. Chu et al. [13] conducted several series of undrained cyclic triaxial tests, involving different cyclic stress ratio, void ratio, loading frequency, and fine particle concentration. Fan et al. [14] used the

discrete element method to study the strength degradation and failure mechanism of soil-rock mixture at different frequencies, dynamic stress amplitudes, and durations. Zhou et al. [15] carried out triaxial tests under different confining pressures on soil-rock mixtures under freeze-thaw cycles. The results show that the rock content and the degree of consolidation are the key factors affecting the elastic modulus of soil-rock mixtures.

Some achievements have been made in the study of the static and dynamic properties of soil-rock mixtures [16–20]. However, there are few studies on the stiffness variation rule of soil-rock mixture under the cyclic load of actual metro trains. Lekarp et al. [21] concluded that the rebound modulus of gravel materials decreases with increasing frequency of metro train loading under saturated undrained conditions. Sun et al. [22, 23] selected the frequency of the metro train load as 5 Hz to 60 Hz and the cyclic stress ratio as 6 to 9 and 3 to 19. The results of the cyclic triaxial test show that the load frequency affects the cumulative deformation of the subgrade filling. Most of the previous studies only considered the influence of factors such as effective consolidation confining pressure, consolidation ratio OCR, cyclic dynamic stress ratio, and vibration frequency of cyclic loading. The impact of the degree of consolidation of soil-rock mixtures was not considered. Moreover, the failure test conducted under a higher cyclic dynamic stress ratio is not consistent with the actual metro train load. Therefore, based on the previous studies, the author investigated the stiffness variation of soil-rock mixture under the actual metro cyclic loading. These tests involved three variables: initial consolidation degree, effective confining pressure, and rock content. Finally, the stiffness softening model of the soil-rock mixture was established based on the cyclic triaxial test data and compared with the field test data. The results of the study can provide a reference for the calculation and control of post-work settlement of metro trains in the backfill area of SRM.

2. Stiffness Softening Test

2.1. Physical Properties of Soil-Rock Mixture and Making Specimen. The samples were taken from Shangwanlu to Huanshan Park on rail line 10 in Yubei District in Chongqing city. According to the Geotechnical Investigation Report for the Section from Shangwanlu to Huanshan Park on Chongqing Rail Transit Line 10, the composition of the soil-rock mixture is silty clay and sandstone. The basic physical parameters are shown in Table 1.

The backfill of the on-site soil-rock mixture contains heavy and large ultradiameter particles (up to 1 m or more). Conventional sieving equipment cannot carry out the test. The original sample is sieved after being scaled down by the equivalent replacement method. The natural gradation curve of the sample particles is shown in Figure 1. The maximum sample size of the DDS-70 electromagnetic vibration triaxial test system is $\Phi 50\,\text{mm} \times 100\,\text{mm}$. The maximum allowable particle size of the sample with a diameter of 50 mm is 5 mm by the Chinese standard (GB/T 50123-2019). Therefore, this article selects a particle size of 2 mm as the soil-rock threshold value of the soil-rock mixture and considers the complete gradation of the fine soil. The gradation of rock is 2~5 mm. The gradation curves of the three groups of soil-rock mixture samples with different rock content are shown in Figure 2.

The experimental work was carried out in strict accordance with the relevant regulations in the Chinese standard (GB/T 50123-2019). The test is divided into 4 steps: sample preparation, saturation, consolidation, and loading.

After the sample is dried, weigh the fine soil and rock of each particle group according to the gradation curve; add water according to the natural moisture content of 9.22%, stir evenly, let it stand, and seal for 24 hours; and then tamp in 5 layers to prepare a $\Phi 50\,\text{mm} \times 100\,\text{mm}$ cylindrical sample with a compaction degree of 0.97. The sample is saturated with stepped back pressure. Each step is increased by 30 kPa. The saturation is completed after the saturation coefficient B value measured under the continuous three-step load reaches 0.95. The sample is shown in Figure 3.

2.2. Test scheme. Figure 3 displays the experimental equipment. The system is composed of four parts: main engine, electric control system, static control cabinet system, and microcomputer system. The main engine mainly includes a vibration exciter and a three-axis chamber.

The test is conducted under the condition of undrained isostatic consolidation. The sign of consolidation completion is that the change of consolidation displacement within 1 h does not exceed 0.1 cm^3. The effective consolidation confining pressure is taken as 100 kPa, 200 kPa, and 400 kPa, respectively. To consider the effect of consolidation degree, the test was conducted by applying the surrounding pressure in stages. The specimens reach different degrees of consolidation before the cyclic load is applied. The degree of consolidation is, respectively, 0.8, 0.9, and 0.98.

Takemiya [24] monitored the metro train operation site in Ledsgard and combined the test results with numerical simulation. It is found that the vibration response frequencies generated by the metro train at low speed (70 km/h) ranged from 0.5 to 1 Hz and 2 to 2.5 Hz, mainly between 0.5 and 1 Hz. Zhang Xi et al. [25] conducted continuous dynamic monitoring on-site for Shanghai Metro Line 2. The monitoring results show that the soil has two response frequencies of 2.4~2.6 Hz and 0.4~0.6 Hz under the metro train load, corresponding to the metro train speed of 30~40 km/h. Chongqing Rail Transit Line 10 uses As-type vehicles. The net axle weight of the As-type train is 150 kN. The length of the metro train is 19.3 m. The maximum operating speed is 100 km/h. The actual operating speed is 60~70 km/h. This article refers to the method of Indraratna et al. [26] to calculate the cyclic load frequency of metro trains.

$$f = \frac{v}{l = 65\text{km/h}/19.3\text{m}} = \frac{18.1\text{m}}{s/19.3\text{m} \approx 1\text{Hz}}. \quad (1)$$

The dynamic stress amplitude is calculated according to the Chinese standard (TB 10001-2016) train dynamic load formula as follows:

Table 1: Summary of physical and mechanical properties of soil-rock mixture backfill.

		Silty clay					Sandstone	
Rock block content (%)	Natural water content (%)	Dry density (kg/m^3)	Specific gravity of soil	Plastic limit (%)	Liquid limit (%)	Plasticity index	Dry density (kg/m^3)	Saturation density (kg/m^3)
43.79	9.22	1700	2.54	17.09	30.16	13.07	2280	2400

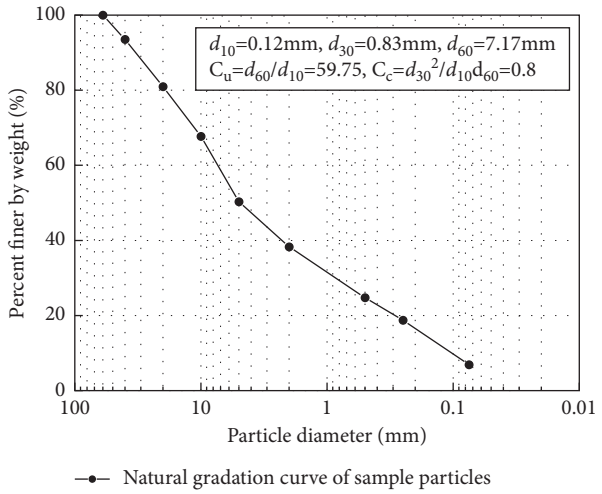

Figure 1: Grading curve of the sample.

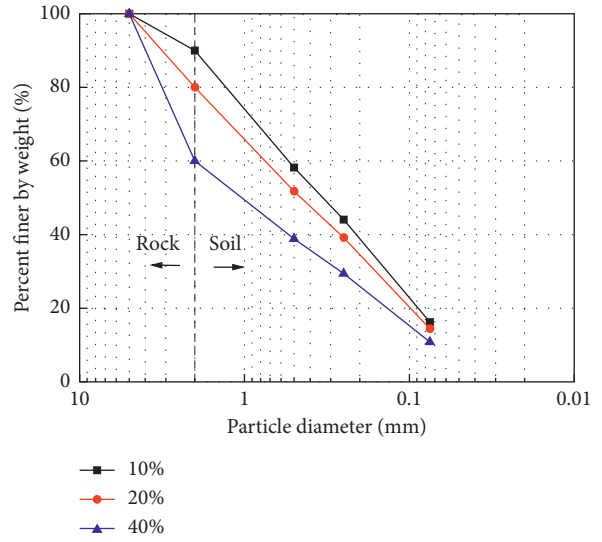

Figure 2: Gradation curves of soil-rock mixture samples with different rock contents.

$$\sigma_d = 0.26 \times P \times (1 + \alpha v) = 0.26 \times 150 \times (1 + 0.003 \times 65) = 46.605\text{kPa}, \quad (2)$$

where σ_d is the amplitude of the design dynamic stress of the railway subgrade (kPa), P is the static axle weight of the metro train (kN), v is the running speed of the metro train (km/h), and α is the speed influence coefficient. The metro train takes 0.003. $1 + \alpha v$ is the impact coefficient.

The soil-rock mixture is compacted under the cyclic load of the metro train, producing vertical displacement, but not vertical expansion. In summary, the cyclic load parameters used in the dynamic triaxial test are rigorously determined according to the actual operational conditions of the Chongqing rail transit. The cyclic load frequency is 1 Hz with a corresponding vehicle speed of 65 km/h. The dynamic stress amplitude is 46 kPa. Sine wave load is biased with a cyclic dynamic stress ratio of 0.12. The number of cycles N is 15,000. The loading mode of the biased sine wave is shown in Figure 4. The relationship curve between the axial strain and

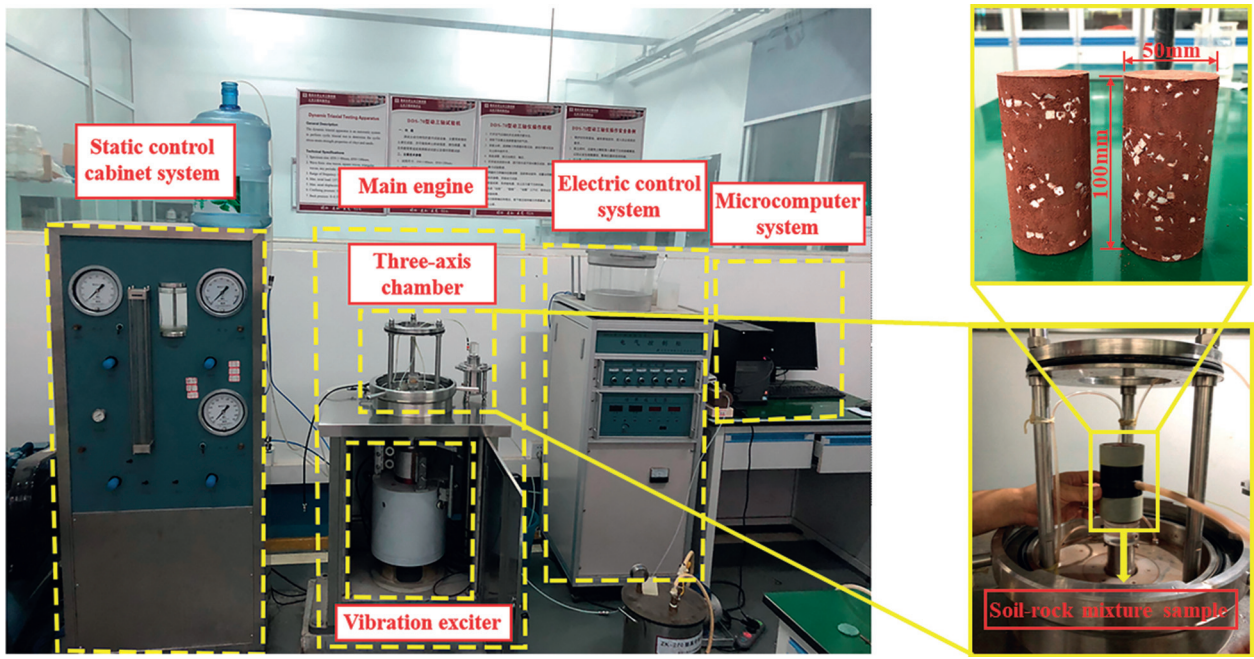

Figure 3: DDS-70 electromagnetic vibration triaxial test system and soil-rock mixture sample.

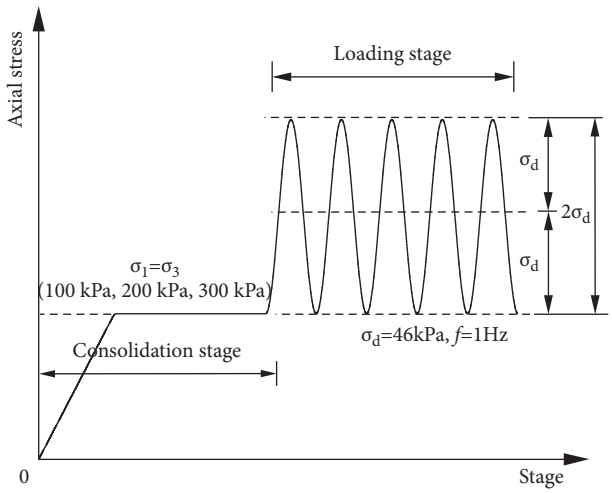

Figure 4: Biased sine wave load.

the number of cycles under the action of the biased sine wave is shown in Figure 5.

This article draws on the method of Hsu et al. [27]. The cyclic load is applied in ten stages. The number of cycles of each level of load is 10 times. The cyclic stress ratio is loaded from 0.01 to 0.1. The cyclic stress ratio of each level differs by 0.01. There is no time interval between different dynamic stress levels. The test scheme of stiffness softening under dynamic load is shown in Table 2.

Specimen groups *A*1–*A*9 are designed to investigate the effects of initial degree of consolidation and effective consolidation confining pressure on the stiffness variation of soil-rock mixtures. Specimen groups *A*10-*A*11 are designed to study the effect of rock content on the change of stiffness of the soil-rock mixture.

3. Experimental Results and Discussion

3.1. Stiffness Softening Index. In this paper, the dynamic triaxial test is stress-controlled. According to the definition of softening index by IDRISS et al. [28] and considering the effect of initial consolidation stress, the softening index is defined as follows:

$$\delta = \frac{G_N}{G_1} = \frac{\left(q_{\max} - q_{\min}/\varepsilon_{N,\max} - \varepsilon_{N,\min}\right)}{\left(q_{\max} - q_{\min}/\varepsilon_{1,\max} - \varepsilon_{1,\min}\right)} = \frac{\varepsilon_{N,\max} - \varepsilon_{N,\min}}{\varepsilon_{1,\max} - \varepsilon_{1,\min}}. \tag{3}$$

In formula (3), G_N and G_1 are the secant modulus of the Nth and 1st cycle hysteresis curves (kPa), $q_{\max}$ and $q_{\min}$ are the maximum and minimum deflection stresses in each cycle (kPa), $\varepsilon_{1,\max}$ and $\varepsilon_{1,\min}$; $\varepsilon_{N,\max}$ and $\varepsilon_{N,\min}$ are the maximum axial strain and minimum axial strain in the 1st and Nth cycles, respectively.

Figure 6 shows the cyclic hysteretic curve of the SRM sample for the 1st, 50th, 100th, 200th, and 300th cycles in the process of strain softening. It can be seen from Figure 6 that the center of the hysteresis curve keeps moving to the right as the number of cycles increases. This indicates that the plastic strain of the soil-rock mixture backfill accumulates gradually under the cyclic loading. The hysteresis curve is sparse on the left and dense on the right, indicating that the strain of the specimen increases rapidly at the beginning of cyclic load loading, and then tends to stabilize.

3.2. The Effect of Initial Consolidation Degree on Stiffness Softening. The curves of the softening index with the number of cycles for different initial consolidation degrees are shown in Figure 7. From the figure, it can be seen that the softening index decays faster at the beginning of loading and

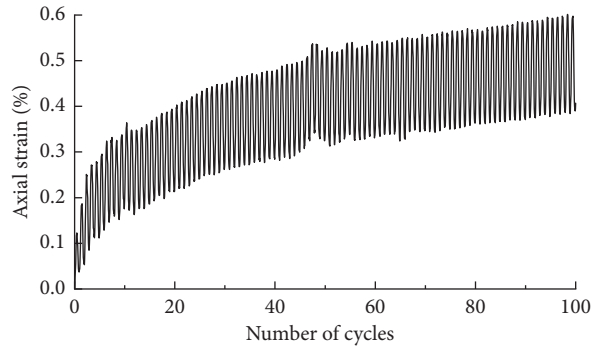

Figure 5: Axial strain versus number of cycles under bias sine wave loading.

tends to stabilize with the increase in the number of cycles. The lower the consolidation degree, the faster the softening index decays and the greater the attenuation amplitude. Figure 8 reflects the effect of consolidation degree on the softening index of the soil-rock mixture at different number of cycles. Figure 8 shows that the consolidation of the soil-rock mixture has a strengthening effect on the stiffness. The increase in the consolidation degree will increase the initial stiffness and stable stiffness of the sample and reduce the loss ratio and relative softening speed.

3.3. The Effect of Effective Consolidation Confining Pressure on Stiffness Softening. Figure 9 reflects the effect of effective consolidation pressure on the softening index of soil-rock mixture under different number of cycles. Figure 9 shows that the lower the effective consolidation confining pressure, the faster the attenuation of the softening index and the greater the attenuation amplitude. The softening index increases as the effective consolidation confining pressure increases (Figure 10). The above law is consistent with the dynamic strength of coarse-grained fill for railroads at different confining pressures. In other words, increasing the confining pressure helps to increase the dynamic stability of the soil-rock mixture.

3.4. The Influence of Rock Content on Stiffness Softening. The rock content is the main factor that affects the mechanical properties of the soil-rock mixture. The effect of rock content on the stiffness of the soil-stone mixture is shown in Figure 11. Figure 11 shows the following. ① In the case of low rock content, the lower the rock content, the faster the attenuation of the softening index and the greater the amplitude. ② With the increase in the rock content, the stiffness changes from softening type to hardening type. The softening index increases with the increase in the number of cycles and finally tends to be stable. This is because when the rock content is higher, the block particles start to contact under the cyclic load forming the backfill skeleton and stiffening of stiffness occurs. ③ There is an inflection point between 20%~40% rock content from softening type to hardening type.

Figure 12 shows the influence of the rock content on the softening index of soil-rock mixture at different number of cycles. It can be seen from Figure 12 that under different number of cycles, the higher the rock content, the greater the softening index. The stable values of the softening index of soil-rock mixture samples under different factors are shown in Table 3.

3.5. Establishment of Stiffness Hardening-Softening Model. With the increase in stone content, the stiffness of soil-stone mixture will be transformed from softened to hardened type. Therefore, it is necessary to model the two different stiffnesses separately. In the existing studies, the stiffness models under cyclic loading are mostly obtained from the simulation analysis of the test results. This paper also established a model between the softening index and the number of cycles through the fitting analysis of the test results.

$$\delta = A + \frac{1}{B + CN} \text{ (the softening type)}, \tag{4}$$

where A, B, and C are experimental fitting parameters. The physical meaning of parameter A is the stable value of the softening index.

The stiffness change law of the soil-rock mixture with higher rock content under metro train loading is similar to that of the stiffness hardening type in this paper. In the initial stage of cyclic load loading, the stiffness of the soil-rock mixture rises quickly with a certain linear relationship. With the increase in the cycle number, the stiffness of the soil-rock mixture tends to be stable. Therefore, this paper only suggests using the segmental function to model the stiffness of soil-rock mixture under high rock content under metro train loading.

$$\delta = \begin{cases} \delta_0 + DN, N \le N_g \\ \delta_w, N > N_g \end{cases} \text{ (the hardening type)}, \tag{5}$$

where δ_0 is the intercept between the fitting line of the softening index cycles curve in the linear stiffness hardening stage and the ordinate axis, δ_1 is the initial softening index value, D is the slope of the curve fitting line of the softening index cycles in the hardening stage, and N_g is the critical number of cycles for the stiffness of the soil-rock mixture to change from hardening to stable. It is the intersection of the increasing straight section and the stable straight section of the stiffness softening index. δ_w is the stable value of the softening index.

Formula (4) is applied to the prediction of the stiffness softening of the soil-rock mixture with a rock content below 20%. Formula (5) is applicable to the prediction of the stiffness hardening of the soil-rock mixture with rock content higher than 40%. The stiffness softening index of the soil-rock mixture is fitted by the empirical model determined by equations (4) and (5). The fitting results are obtained as shown in Figures 13 and 14. Table 4 shows the statistics of fitting parameters. The fitting degree is above 0.9.

Table 2: Stiffness softening test program.

Specimen group	Rock content (%)	Compaction coefficient	Consolidation degree	Consolidation stress (kPa)	Cyclic stress ratio	Cycles	f(Hz)
$A1$	20	0.97	0.98	100	0.12	15000	1
$A2$	20	0.97	0.90	100	0.12	15000	1
$A3$	20	0.97	0.80	100	0.12	15000	1
$A4$	20	0.97	0.98	200	0.12	15000	1
$A5$	20	0.97	0.90	200	0.12	15000	1
$A6$	20	0.97	0.80	200	0.12	15000	1
$A7$	20	0.97	0.98	400	0.12	15000	1
$A8$	20	0.97	0.90	400	0.12	15000	1
$A9$	20	0.97	0.80	400	0.12	15000	1
$A10$	10	0.97	0.98	200	0.12	15000	1
$A11$	40	0.97	0.98	200	0.12	15000	1

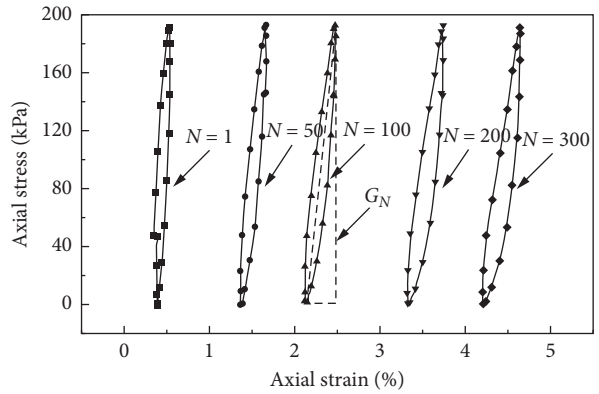

Figure 6: Hysteresis curve of strain softening ($P = 20\%, U = 0.80, \sigma_3' = 400kPa$).

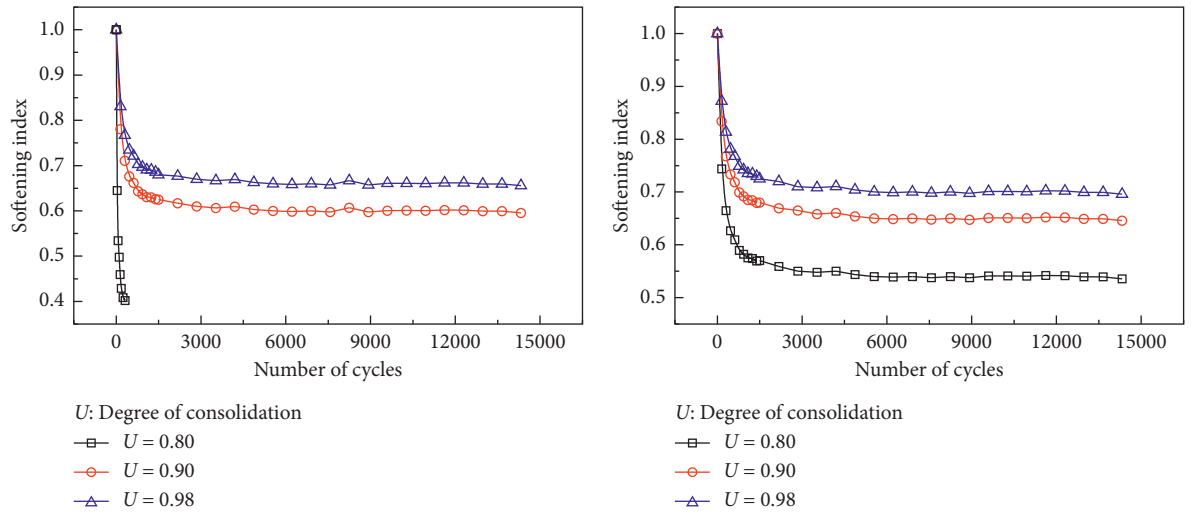

Figure 7: Continued.

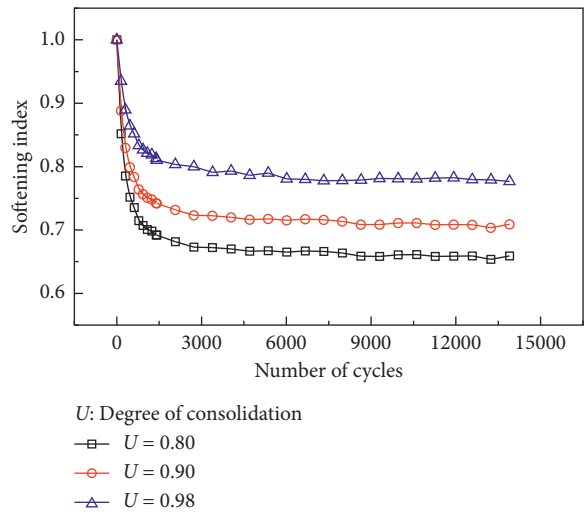

(c)

Figure 7: Degree of consolidation effect on the softening index of SRM: (a) $P = 20\%$ and $\sigma_3' = 100$kPa; (b) $P = 20\%$ and $\sigma_3' = 200$kPa; (c) $P = 20\%$ and $\sigma_3' = 400$kPa.

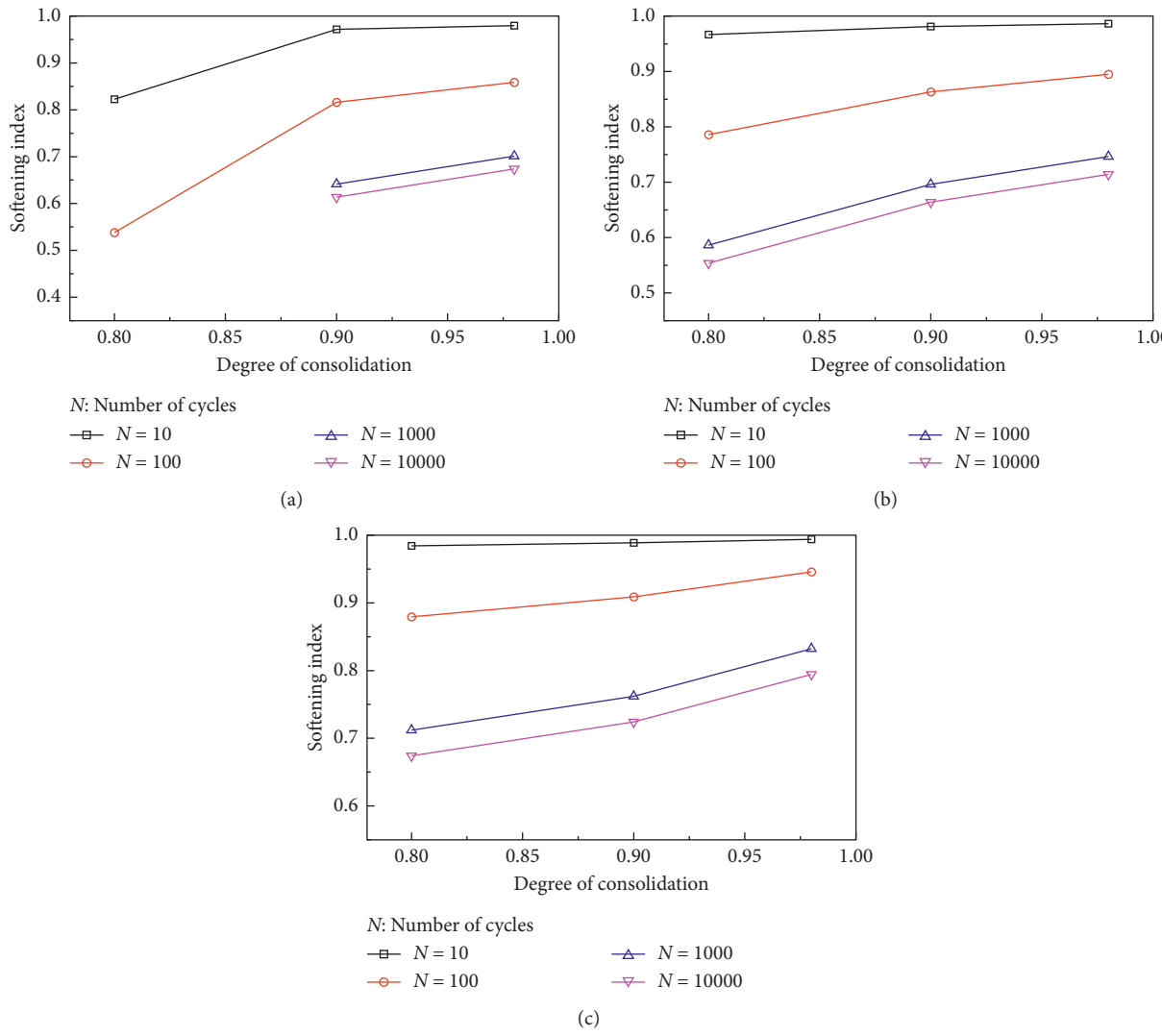

Figure 8: Curve of degree of consolidation and softening index under different number of cycles: (a) $P = 20\%$ and $\sigma_3' = 100$kPa; (b) $P = 20\%$ and $\sigma_3' = 200$kPa; (c) $P = 20\%$ and $\sigma_3' = 400$kPa.

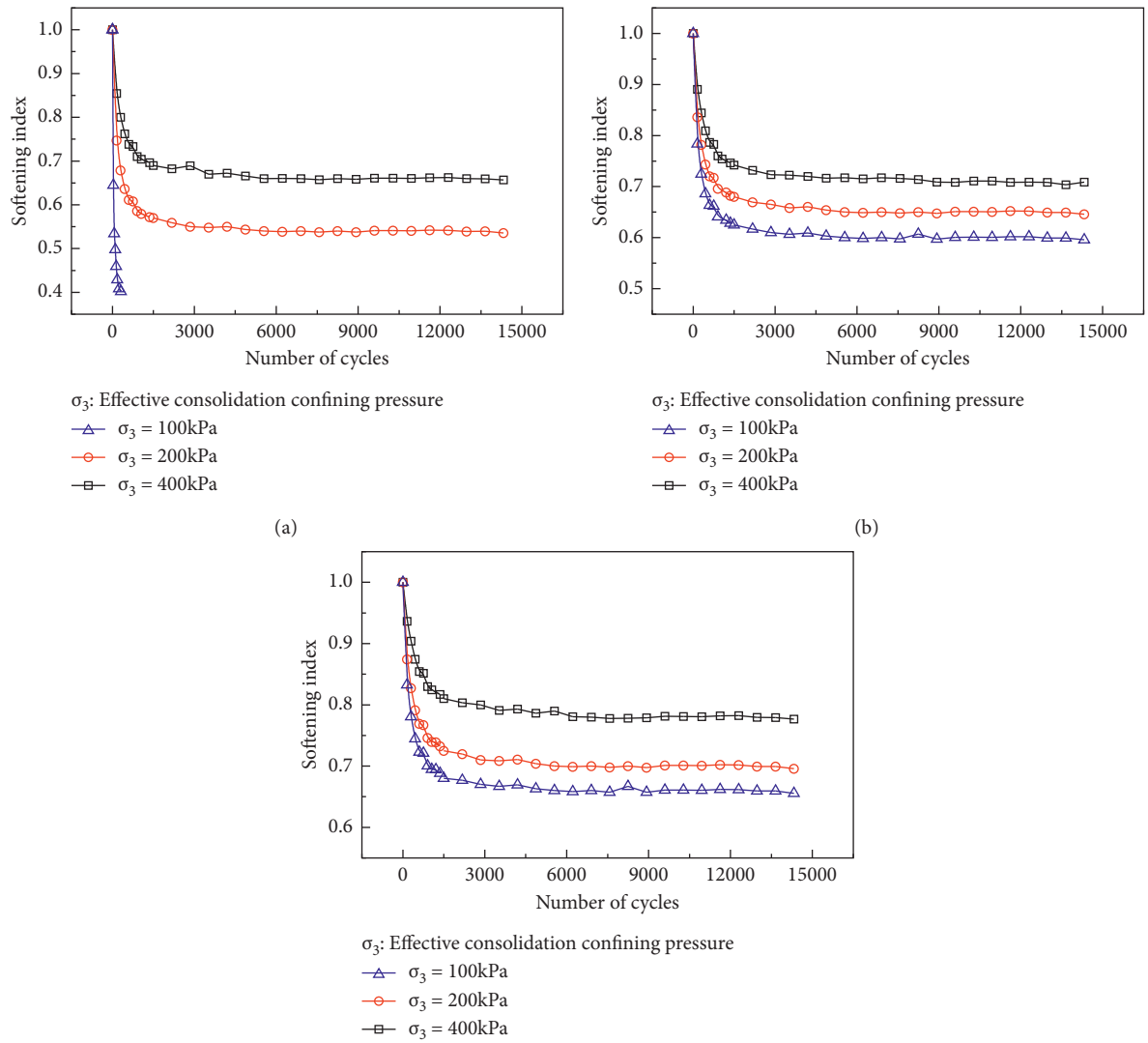

Figure 9: Effective confirming pressures effect on the softening index of SRM: (a) $P = 20\%$ and $U = 0.80$; (b) $P = 20\%$ and $U = 0.90$; (c) $P = 20\%$ and $U = 0.98$.

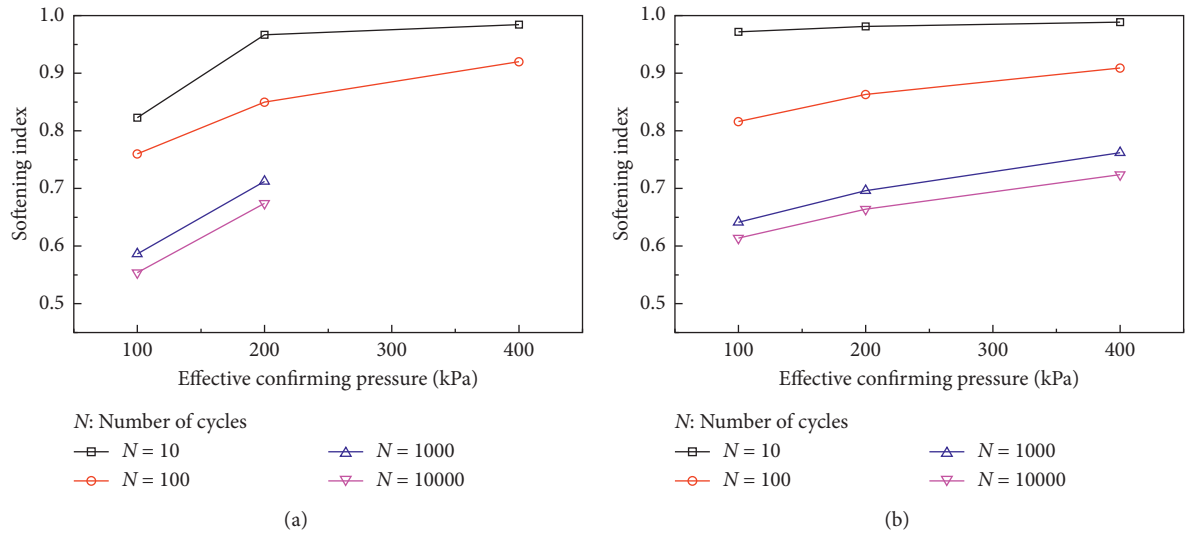

Figure 10: Continued.

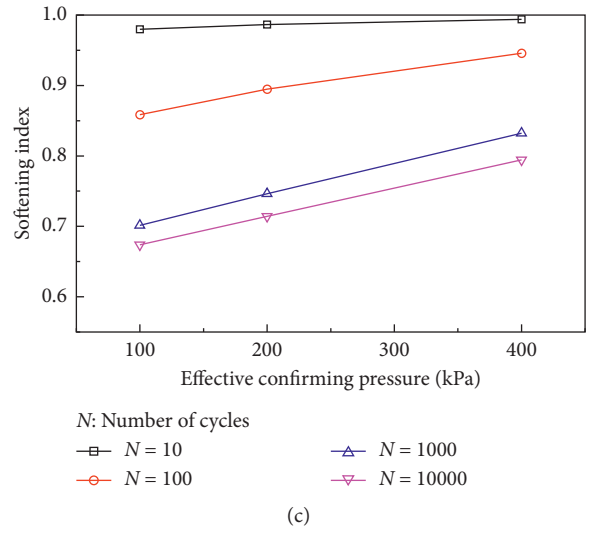

Figure 10: Curve of effective confirming pressures and softening index under different number of cycles: (a) $P = 20\%$ and $U = 0.80$; (b) $P = 20\%$ and $U = 0.90$; (c) $P = 20\%$ and $U = 0.98$.

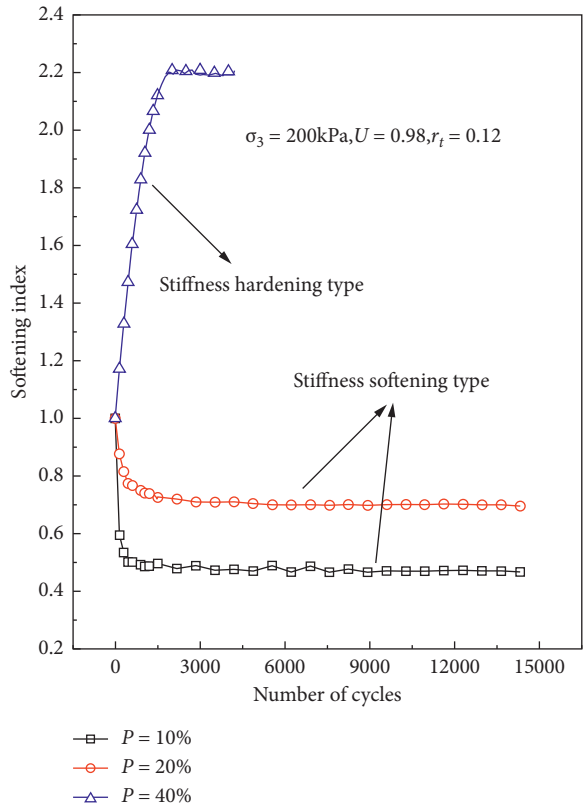

Figure 11: Rock content effect on the softening index of SRM.

To verify the accuracy of the soil-rock mixture backfill stiffness and softening model established based on the experimental data, we conducted field tests on the shear wave velocity of the soil in the section from Shangwanlu to Huanshan Park on Chongqing Rail Transit Line 10. Table 5 shows the results of the shear wave test of the backfilled soil on-site. By the Chinese standard (GB/T 50266-2013), the dynamic stiffness can be calculated with the following formula:

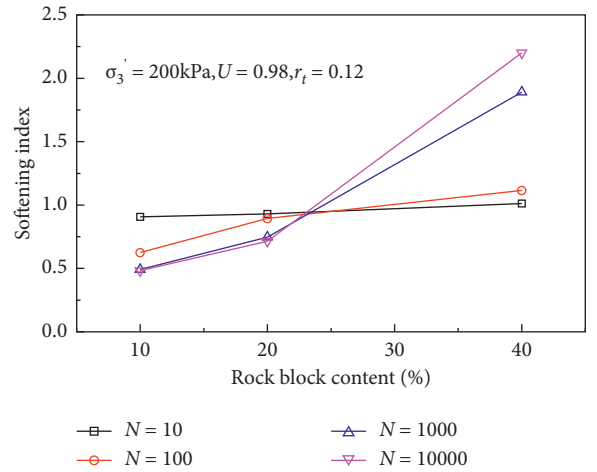

Figure 12: Curve of rock content and softening index under different number of cycles.

$$E_d = \frac{\rho v_s^2\left(3v_p^2 - 4v_s^2\right)}{v_p^2 - v_s^2} = 2\rho v_s^2(1+\mu)\times 10^{-3}, \quad \delta = \frac{E_{d2}}{E_{d1}} = \frac{v_{s2}^2}{v_{s1}^2}, \tag{6}$$

where E_d is the dynamic stiffness (MPa), μ is Poisson's ratio, ρ is the density (kg/m^3), v_p is the compression wave velocity (m/s), and v_s is the shear wave velocity (m/s).

The shear wave velocities of the plain fill before and after the metro train is opened are 213 m/s and 322 m/s. The dynamic stiffness hardening index is 2.29. The measured value of stiffness change is basically consistent with the stiffness hardening model established based on the stiffness change data of the specimen with a rock content of 40%. The corresponding softening index is 2.20 (the rock content of the on-site backfill is 40%~50%).

Table 3: Impact of various factors on the softening index.

Rock content (%)	Consolidation stress (kPa)	Consolidation degree	Stability softening index
		0.98	0.78
	100	0.90	0.71
		0.80	0.66
		0.98	0.70
20	200	0.90	0.65
		0.80	0.54
		0.98	0.66
	400	0.90	0.60
		0.80	<0.40 (breaking)
10	200	0.98	0.47
40	200	0.98	2.20 (hardening)

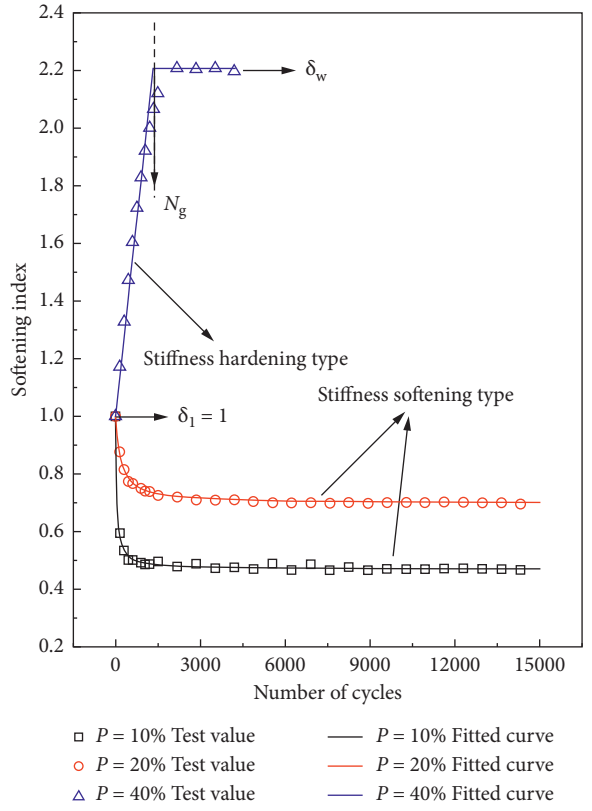

Figure 13: Fitting value of the evolution of the softening index under different rock contents.

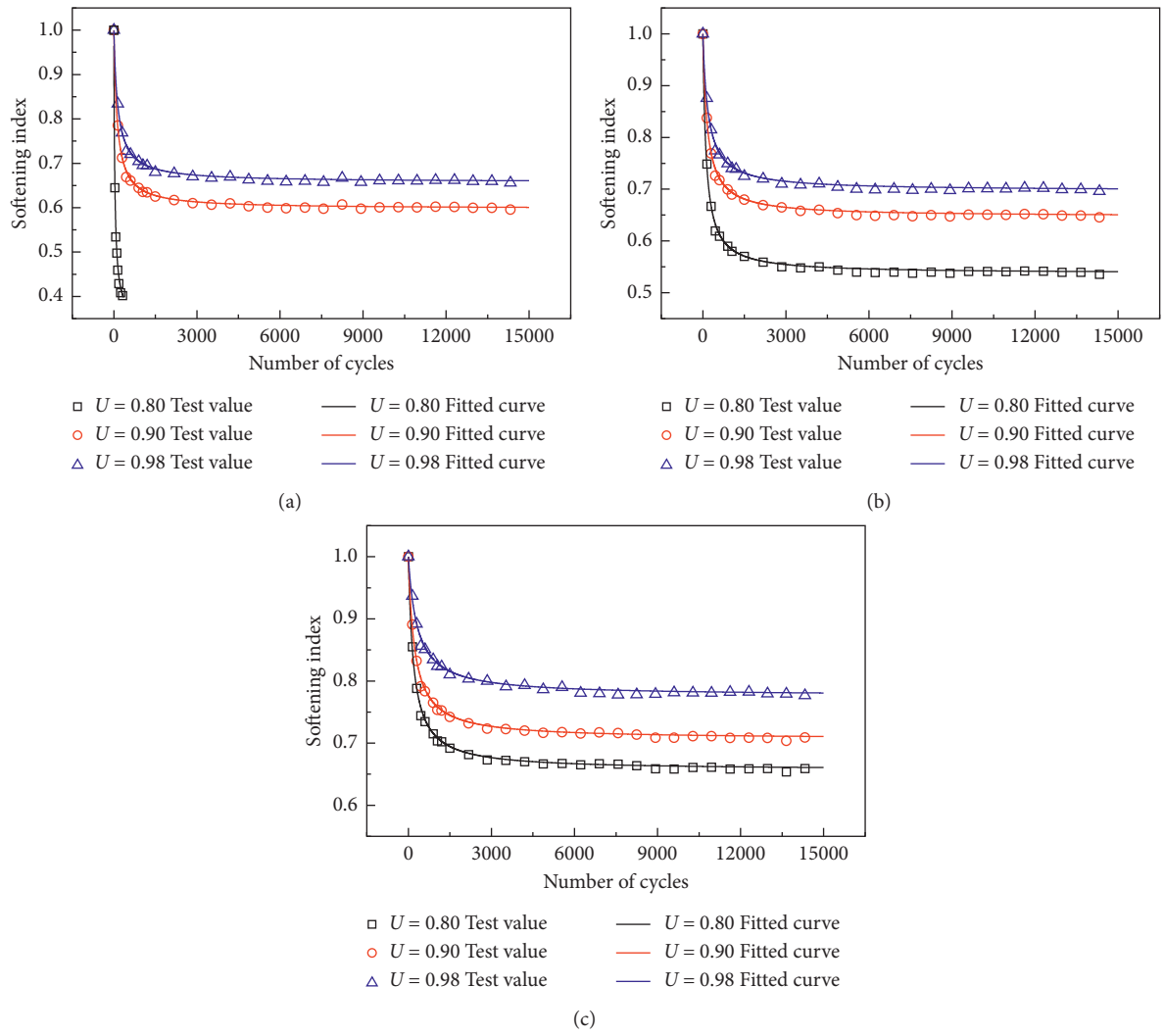

Figure 14: The fitting value of the development of the softening index under different degrees of consolidation: (a) $P = 20\%$ and $\sigma_3' = 100$kPa; (b) $P = 20\%$ and $\sigma_3' = 200$kPa; (c) $P = 20\%$ and $\sigma_3' = 400$kPa.

Table 4: Fitting parameters of the stiffness softening model.

Rock content (%)	Consolidation stress (kPa)	Consolidation degree	A	B	C	R^2
20	100	0.98	0.7760	4.4490	0.0139	0.9340
		0.90	0.7063	3.3910	0.0150	0.9491
		0.80	0.6565	2.8960	0.0156	0.9564
	200	0.98	0.6969	3.2820	0.0172	0.9457
		0.90	0.6470	2.8160	0.0177	0.9532
		0.80	0.5371	2.1440	0.0185	0.9643
	400	0.98	0.6574	2.9000	0.0202	0.9463
		0.90	0.5975	2.4650	0.0207	0.9542
		0.80	0.3364	1.5500	0.0422	0.9800
10	200	0.98	0.5592	0.4200	0.0030	0.9961
40	200	0.98		$\delta_0 = 0.9991$; $D = 0.0009$ $Ng = 1335$; $\delta_w = 2.2068$		

Table 5: Shear wave velocity test results.

Working condition	Test hole number	Test range (m)	Lithology	v_s (m/s)	Equivalent shear wave velocity (m/s)
Before the metro train opened	SHXK14	0~50	Plain fill	205~231	213
		50~52	Sandstone	623~1244	
	SHXK15	0~60	Plain fill	201~225	
		60~62	Sandstone	658~1234	
13 months after the metro train opened	138-7	0~27	Plain fill	315~337	322
	204-6	0~27	Plain fill	330~348	

4. Conclusions

In this study, the effect of the initial consolidation degree, the effective consolidation confining pressure, and the rock content upon the stiffness softening of the soil-rock mixture was studied according to the cyclic load dynamic triaxial test. The following conclusions were drawn:

(1) Both the initial consolidation degree and the effective consolidation confining pressure can affect the stiffness softening of the soil-rock mixture. The softening index stable value of SRM increases with the increase in initial consolidation degree and the effective consolidation confining pressure.

(2) The stiffness of the SRM changes from softening to hardening with the increase in rock content. The critical range of stiffness softening and hardening is 20% to 40%. The softening index stable value of SRM increases with the increase in rock content. For the type of softening, the softening index decreases as the number of cycles increases, and ultimately tends to be stable. For the type of hardening, the softening index increases approximately linearly at the beginning of loading and eventually tends to be stable as well.

(3) A stiffness softening and hardening model for SRM was proposed based on the cyclic load dynamic triaxial test, and the shear wave velocity test results were in good agreement with the cyclic load dynamic triaxial test results, which indicated that the stiffness softening and hardening models can be used to describe the dynamic behavior of SRM well.

(4) The dynamic stiffness change of the soil-rock mixture can reflect the constitutive relationship between its stress and strain, and it is also a key indicator for predicting and analyzing the cumulative deformation of the soil-rock mixture. The results of the study can provide a reference for the calculation and control of post-work settlement of metro trains in the backfill area of SRM.

Data Availability

The data used to support the findings of this study are available from the corresponding author upon request.

Conflicts of Interest

The authors declare that they have no conflicts of interest regarding the publication of this paper.

Authors' Contributions

Zuliang Zhong, Hong Zou, and Xiangxiang Hu designed the test scheme. Zuliang Zhong and Xiangxiang Hu performed the tests. Hong Zou and Xinrong Liu analyzed the test data. Zuliang Zhong and Hong Zou wrote the paper. All authors have read and agreed to the published version of the manuscript.

Acknowledgments

The work described in this paper was supported by the National Natural Science Foundation of China (No. 52074042).

References

[1] N. Li, X. Wang, R. Qiao et al., "A prediction model of permanent strain of unbound gravel materials based on performance of single-size gravels under repeated loads," *Construction and Building Materials*, vol. 246, Article ID 118492, 2020.

[2] Q. Huang, H. Huang, B. Ye, D. Zhang, and F. Zhang, "Evaluation of train-induced settlement for metro tunnel in saturated clay based on an elastoplastic constitutive model," *Underground Space*, vol. 3, no. 2, pp. 109–124, 2018.

[3] X. Z. Ling, P. Li, F. Zhang, Y. Zhao, Y. Li, and L. An, "Permanent deformation characteristics of coarse grained subgrade soils under train-induced repeated load," *Advances in Materials Science and Engineering*, vol. 2017, Article ID 6241479, 15 pages, 2017.

[4] M. Paul, K. Bakshi, and R. B. Sahu, "An analytical model for radial consolidation prediction under cyclic loading," *Geomechanics and Engineering*, vol. 26, no. 4, pp. 333–343, 2021.

[5] D. R. Panique Lazcano, R. Galindo Aires, and H. Patiño Nieto, "Bearing capacity of shallow foundation under cyclic load on cohesive soil," *Computers and Geotechnics*, vol. 123, Article ID 103556, 2020.

[6] T. Wichtmann, A. Niemunis, and T. Triantafyllidis, "Strain accumulation in sand due to cyclic loading: drained triaxial tests," *Soil Dynamics and Earthquake Engineering*, vol. 25, no. 12, pp. 967–979, 2005.

[7] L. Guo, J. Wang, Y. Cai, H. Liu, Y. Gao, and H. Sun, "Undrained deformation behavior of saturated soft clay under long-term cyclic loading," *Soil Dynamics and Earthquake Engineering*, vol. 50, pp. 28–37, 2013.

[8] M. Bayat, "Effect of sand fouling on the dynamic properties and volume change of gravel during cyclic loadings," *Periodica Polytechnica: Civil Engineering*, vol. 64, no. 3, pp. 741–750, 2020.

[9] A. S. J. Suiker, E. T. Selig, and R. Frenkel, "Static and cyclic triaxial testing of ballast and subballast," *Journal of*

Geotechnical and Geoenvironmental Engineering, vol. 131, no. 6, pp. 771–782, 2005.

[10] J. Lackenby, B. Indraratna, G. McDowell, and D. Christie, "Effect of confining pressure on ballast degradation and deformation under cyclic triaxial loading," *Géotechnique*, vol. 57, no. 6, pp. 527–536, 2007.

[11] S. Lenart, J. Koseki, Y. Miyashita, and T. Sato, "Large-scale triaxial tests of dense gravel material at low confining pressures," *Soils and Foundations*, vol. 54, no. 1, pp. 45–55, 2014.

[12] Z. M. He, Y. X. Liu, H. L. Tang, Y. H. Xing, and H. B. Bian, "Experimental study on cumulative plastic deformation of coarse-grained soil high-grade roadbed under long-term vehicle load," *Advances in Civil Engineering*, vol. 2018, Article ID 8167205, 8 pages, 2018.

[13] M.-C. Chu and L. Ge, "Stiffness degradation of coarse and fine sand mixtures due to cyclic loading," *Engineering Geology*, vol. 288, Article ID 106155, 2021.

[14] Y. B. Fan, O. I. Adewuyi, and F. Chun, "Strength characteristics of soil rock mixture under equal stress and cyclic loading conditions," *Geosystem Engineering*, vol. 18, no. 1, pp. 73–77, 2015.

[15] Z. Zhou, Z.-Z. Liu, H. Yang, W.-Y. Gao, and C.-C. Zhang, "Freeze-thaw damage mechanism of elastic modulus of soil-rock mixtures at different confining pressures," *Journal of Central South University*, vol. 27, no. 2, pp. 554–565, 2020.

[16] S. S. Sharma and M. Fahey, "Degradation of stiffness of cemented calcareous soil in cyclic triaxial tests," *Journal of Geotechnical and Geoenvironmental Engineering*, vol. 129, no. 7, pp. 619–629, 2003.

[17] M. K. Jafari and A. Shafiee, "Mechanical behavior of compacted composite clays," *Canadian Geotechnical Journal*, vol. 41, no. 6, pp. 1152–1167, 2004.

[18] S. R. Sun, F. Zhu, J. H. Wei, W. C. Wang, and H. L. Le, "Experimental study on shear failure mechanism and the identification of strength characteristics of the soil-rock mixture," *Shock and Vibration*, vol. 2019, Article ID 7450509, 25 pages, 2019.

[19] S. N. Wang, T. T. Ji, Q. P. Xue, Z. F. Shen, and Q. Zhang, "Deformation and failure characteristics of soil-rock mixture considering material composition and random structure," *Advances in Materials Science and Engineering*, vol. 2019, Article ID 3165096, 13 pages, 2019.

[20] Y. Su, Y.-J. Cui, J.-C. Dupla, and J. Canou, "Effect of water content on resilient modulus and damping ratio of fine/coarse soil mixtures with varying coarse grain contents," *Transportation Geotechnics*, vol. 26, Article ID 100452, 2021.

[21] F. Lekarp, U. Isacsson, and A. Dawson, "State of the art. I: resilient response of unbound aggregates," *Journal of Transportation Engineering*, vol. 126, no. 1, pp. 66–75, 2000.

[22] Q. D. Sun, B. Indraratna, and S. Nimbalkar, "Effect of cyclic loading frequency on the permanent deformation and degradation of railway ballast," *Géotechnique*, vol. 64, no. 9, pp. 746–751, 2014.

[23] Q. D. Sun, B. Indraratna, and S. Nimbalkar, "Deformation and degradation mechanisms of railway ballast under high frequency cyclic loading," *Journal of Geotechnical and Geoenvironmental Engineering*, vol. 142, no. 1, Article ID 4015056, 2016.

[24] H. Takemiya, "Simulation of track-ground vibrations due to a high-speed train: the case of X-2000 at Ledsgard," *Journal of Sound and Vibration*, vol. 261, no. 3, pp. 503–526, 2003.

[25] X. Zhang, Y. Tang, N. Zhou, J. Wang, and S. Zhao, "Dynamic response of saturated soft clay around a subway tunnel under vibration load," *Tumu Gongcheng Xuebao/China Civil Engineering Journal*, vol. 40, no. 2, pp. 85–88, 2007.

[26] B. Indraratna, S. Nimbalkar, and C. Rujikiatkamjorn, "From theory to practice in track geomechanics - Australian perspective for synthetic inclusions," *Transportation Geotechnics*, vol. 1, no. 4, pp. 171–187, 2014.

[27] C.-C. Hsu and M. Vucetic, "Threshold shear strain for cyclic pore-water pressure in cohesive soils," *Journal of Geotechnical and Geoenvironmental Engineering*, vol. 132, no. 10, pp. 1325–1335, 2006.

[28] I. M. Idriss, R. Dobry, and R. D. Singh, "Nonlinear behavior of soft clays during cyclic loading," *Journal of the Geotechnical Engineering Division*, vol. 104, no. 12, pp. 1427–1447, 1978.